Supporting Information

Saturated Vapor-assisted Growth of Single-Crystalline Organic-Inorganic Hybrid Perovskite Nanowires for High-performance Photodetectors with Robust Stability

Xiuzhen Xu, Xiujuan Zhang, Wei Deng, Liming Huang, Wei Wang, Jiansheng Jie* and Xiaohong Zhang*

*E-mail: jsjie@suda.edu.cn, xjzhang@suda.edu.cn

Institute of Functional Nano & Soft Materials (FUNSOM), Collaborative Innovation Center of Suzhou Nano Science and Technology (NANO-CIC), Jiangsu Key Laboratory for Carbon-Based Functional Materials & Devices, Soochow University, Suzhou Jiangsu 215123, P. R. China.

Table S1: Comparison of the preparation methods, crystal qualities, growth atmospheres, and morphologies of the perovskite NWs in this work with these in literatures.

Materials	**Methods**	**Growth atmospheres**	**Grain boundaries/ surface defects**	**Morphologies**	**Ref**
$CH_3NH_3PbI_3$ NW	One-step	Organic solvent vapor	Few	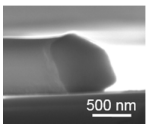	Our work
$CH_3NH_3PbI_3$ NW	Template-assisted one-step method	Organic solvent vapor	Few	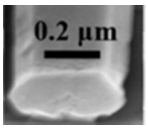	1
$CH_3NH_3PbI_3$ NW	Two-step	CH_3NH_3I vapor	Many	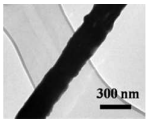	2
$CH_3NH_3PbI_3$ NW	One-step	Air	Many	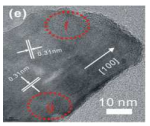	3
$CH_3NH_3PbI_3$ NW	One-step	Air	Many	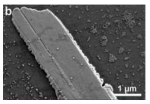	4
$CH_3NH_3PbI_3$ NW	Two-step	Solution	Few	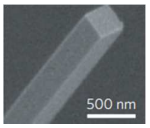	5
$CH_3NH_3PbBr_3$ porous NW	Two-step	Organic solvent	Many	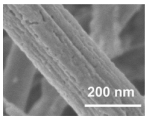	6

Table S2. As-grown $CH_3NH_3PbI_3$ NWs with different concentrations.

Concentration (mol/L)	0.0025	0.005	0.0075	0.01
Average size (nm)	500	580	910	1100

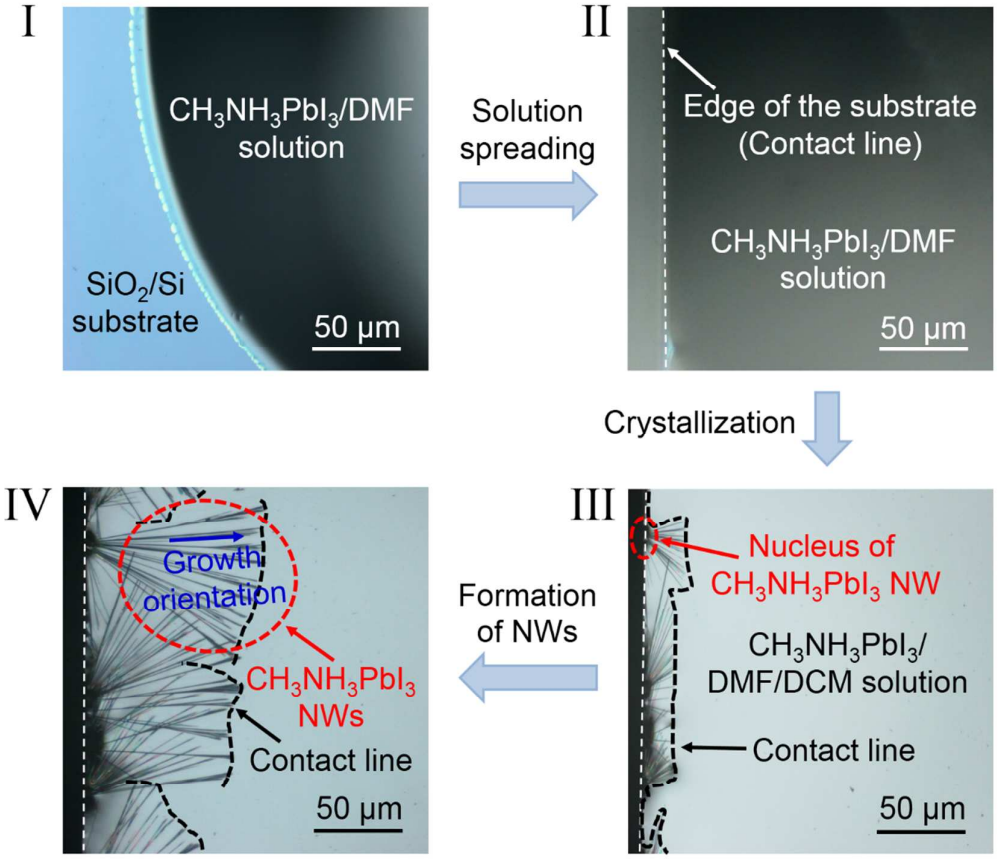

Figure S1. In situ observation of the $CH_3NH_3PbI_3$ NWs growth process.

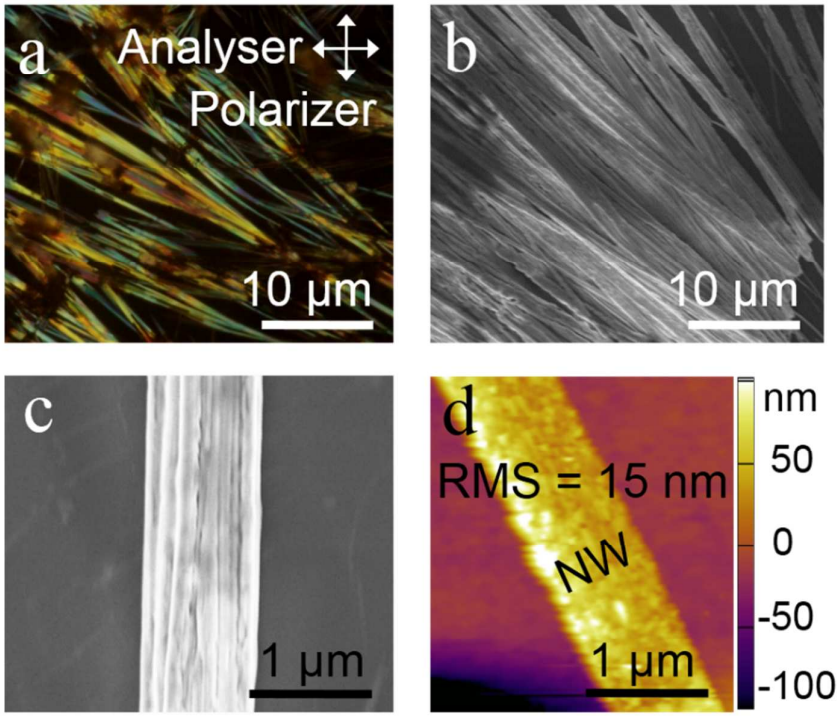

Figure S2. (a) Cross-polarized optical micrograph of the $CH_3NH_3PbI_3$ NWs grown in ambient air. (b) SEM image of the $CH_3NH_3PbI_3$ NWs grown in ambient air. (c) Magnified SEM image of the $CH_3NH_3PbI_3$ NW grown in ambient air. (d) AFM image of the $CH_3NH_3PbI_3$ NW grown in ambient air.

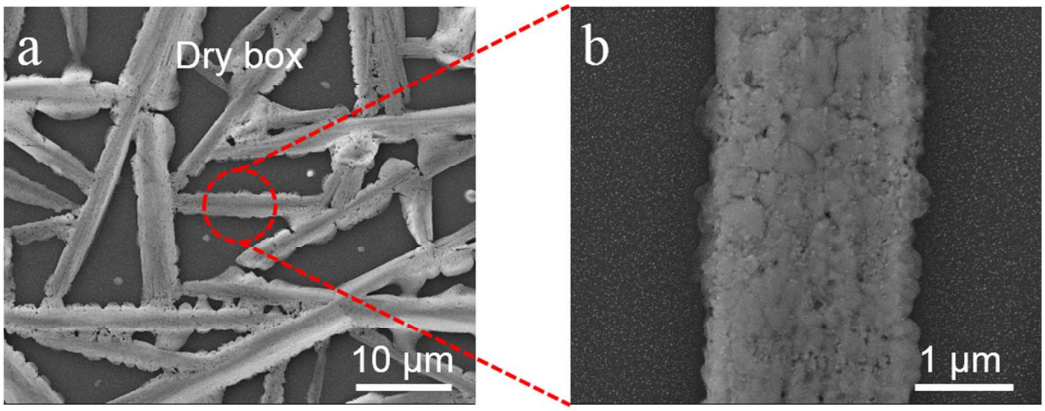

Figure S3. (a, b) SEM images of the $CH_3NH_3PbI_3$ NWs grown in dry box (humidity ~15%).

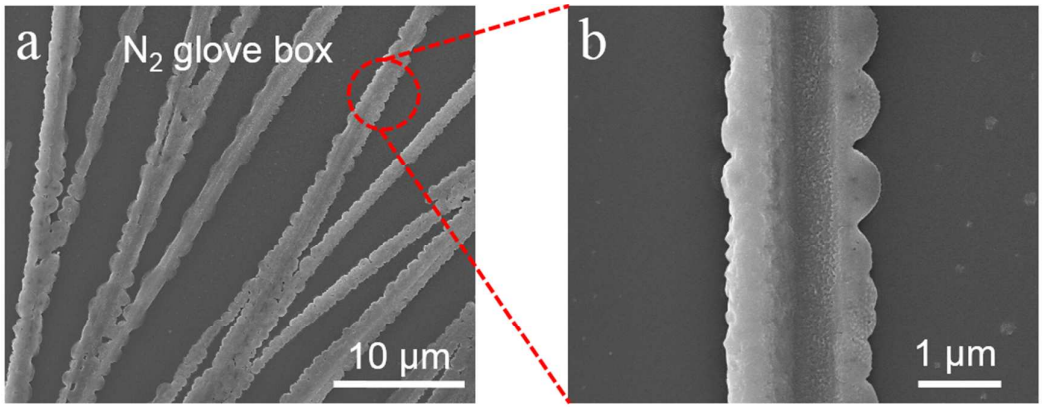

Figure S4. (a, b) SEM images of the $CH_3NH_3PbI_3$ NWs grown in N_2 glove box.

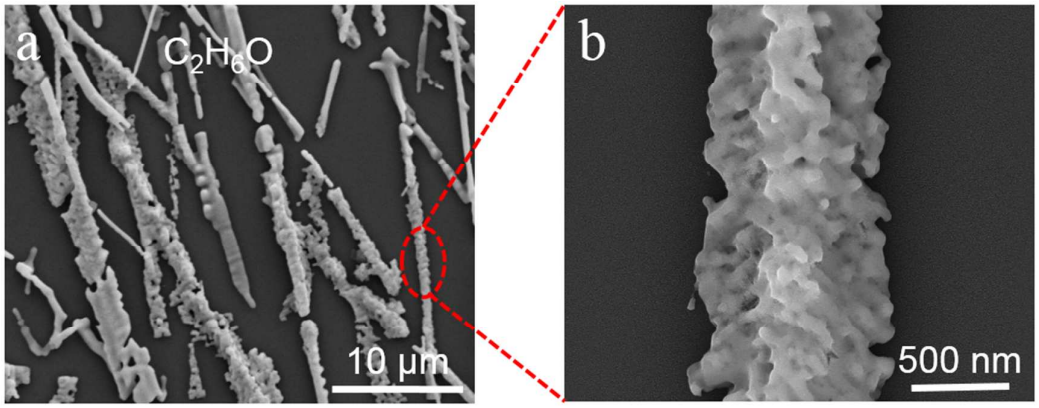

Figure S5. (a, b) SEM images of the $CH_3NH_3PbI_3$ NWs grown in ethanol vapor atmosphere.

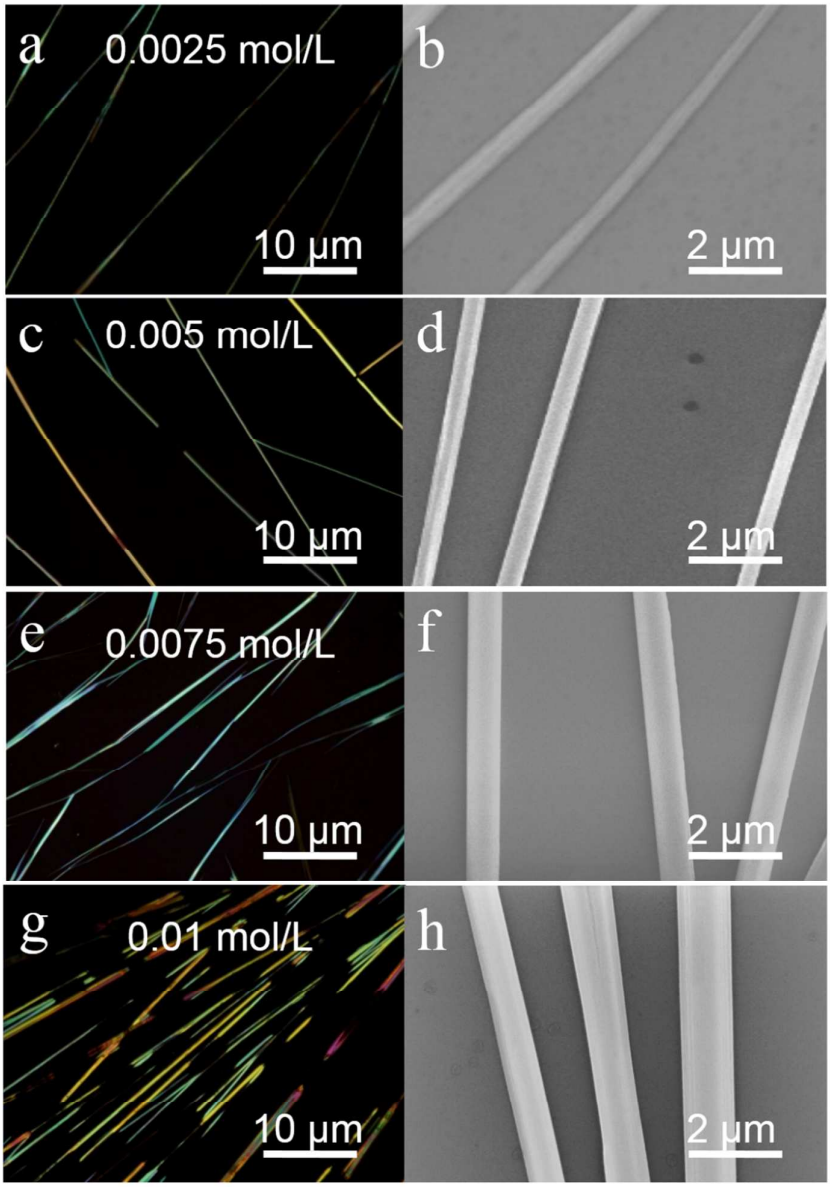

Figure S6. Optical and SEM images of as-grown $CH_3NH_3PbI_3$ NWs with different concentrations: (a, b) 0.0025 mol/L, (c, d) 0.005 mol/L, (e, f) 0.0075 mol/L, and (g, h) 0.01 mol/L.

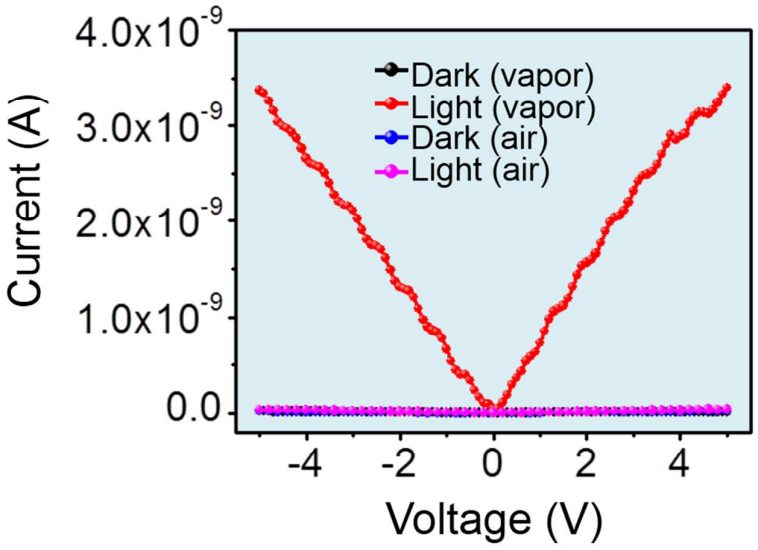

Figure S7. Dark/photo current of the photodetector based on $CH_3NH_3PbI_3$ NW synthesized under saturated vapor and in ambient air, respectively. The light intensity was fixed at 60 μW/cm^2.

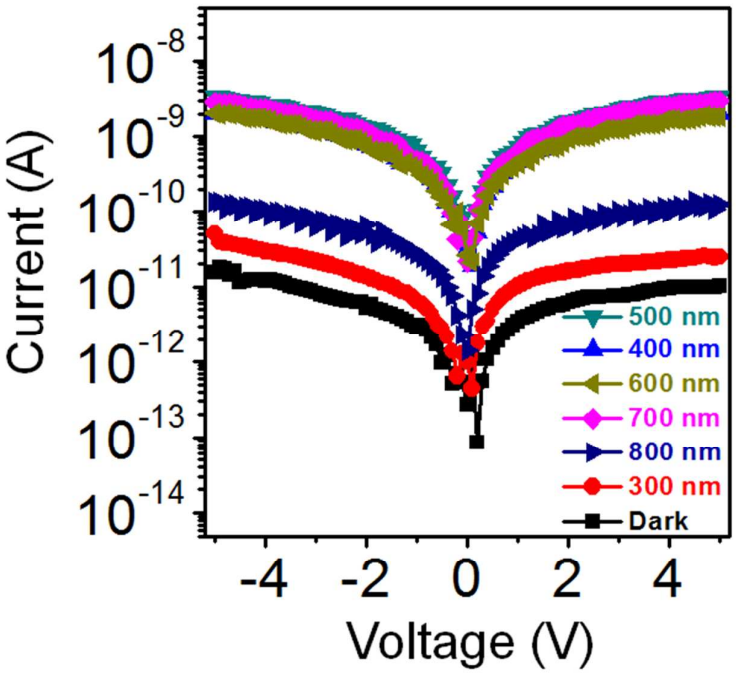

Figure S8. *I-V* curves of the photodetector measured in the dark and under illumination with a different wavelength. The light intensity was fixed at 60 μW/cm^2.

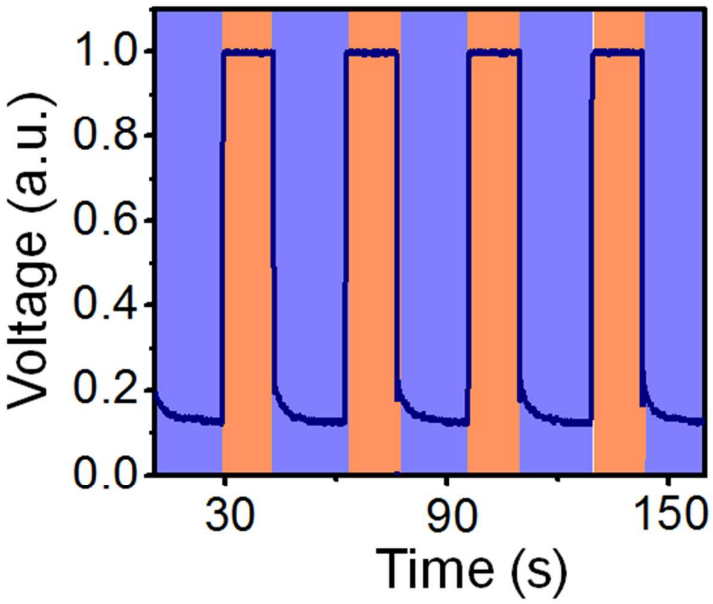

Figure S9. Time-resolved photoresponse of the $CH_3NH_3PbI_3$ NW-based photodetector. The 600 nm-light source was turned on/off by a signal generator to generate pulsed light.

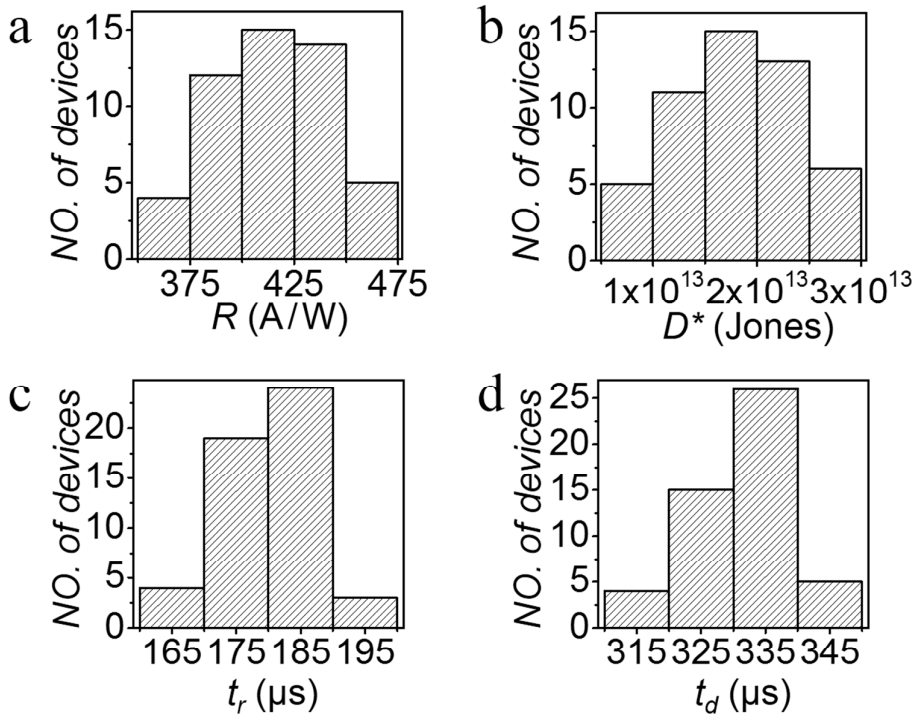

Figure S10. (a-d) Histograms of R, D^*, t_r and t_d measured from 50 devices under the same conditions (460 nm, 60 μW/cm^2).

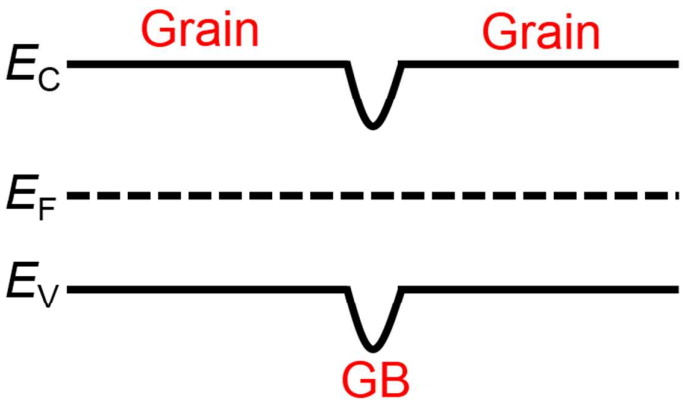

Figure S11. Band alignment between grains and GB.

Photoresponsivity of the photodetector is calculated by the following equation:

$$R_\lambda = \frac{J_{ph} - J_d}{L_{light}} = \frac{I_{light} - I_{dark}}{A \times L_{light}}$$

where I_{light} is the photo-generated current under light illumination, I_{dark} is the current in dark, A is the active area ($A = W \times L$, where W is the width of the NW, L is the channel length of the device) of the photodetector, and L_{light} is the light intensity. In this case, I_{light} and I_{dark} for the single $CH_3NH_3PbI_3$ NW at light wavelength of 460 nm were measured to be 3.37×10^{-9} and 1.57×10^{-11} A, respectively. Active area for the $CH_3NH_3PbI_3$ NW-based device was ~1.215×10^{-7} cm^2 (W is 0.45 μm and L is 27 μm). The light intensity for the incident light was fixed at 60 μW/cm^2, which was calibrated with a silicon photodiode (Newport, 918D-UV-OD3R). Thus the highest R value was estimated to be 460 A/W at an incident light wavelength of 460 nm.

REFERENCES

(1) Deng, W.; Huang, L. M.; Xu, X. Z.; Zhang, X. J; Jin, X. C.; Lee, S. T.; Jie, J. S., *Nano Lett.* **2017**, *17*, 2482-2489.

(2) Gu, L. L.; Tavakoli, M. M.; Zhang, D. Q.; Zhang, Q. P.; Waleed, A.; Xiao, Y. Q; Tsui, K. H.; Lin, Y. J.; Liao, L.; Wang, J. N.; Fan, Z. Y., *Adv. Mater.* **2016**, *28*, 9713-9721.

(3) Deng, H.; Dong, D. D.; Qiao, K. K.; Bu, L. L.; Li, B.; Yang, D.; Wang, H. E.; Cheng, Y. B.; Zhao, Z. X.; Tang, J.; Song, H. S., *Nanoscale* **2015**, *7*, 4163-4170.

(4) Horváth, E.; Spina, M.; Szekrényes, Z.; Kamarás, K.; Gaal, R.; Gachet, D.; Forró, L., *Nano Lett.* **2014**, *14*, 6761-6766.

(5) Zhu, H. M.; Fu, Y. P.; Meng, F.; Wu, X. X.; Gong, Z. Z.; Ding, Q.; Gustafsson,

M. V.; Trinh, M. T.; Jin, S.; Zhu, X. Y., *Nat. Mater.* **2015**, *14*, 636-642.

(6) Zhuo, S. F.; Zhang, J. F.; Shi, Y. M.; Huang, Y.; Zhang, B., *Angew. Chem. Int. Ed.* **2015**, *54*, 5693-5696.